Journal of Zhejiang University-SCIENCE A (Applied Physics & Engineering)
ISSN 1673-565X (Print); ISSN 1862-1775 (Online)
www.zju.edu.cn/jzus; www.springerlink.com
E-mail: jzus@zju.edu.cn

Bending behavior of double-row stabilizing piles with constructional time delay*

Yang YU[1], Yue-quan SHANG[1], Hong-yue SUN[†‡2]

([1]*College of Civil Engineering and Architecture, Zhejiang University, Hangzhou 310058, China*)

([2]*Department of Ocean Science and Engineering, Zhejiang University, Hangzhou 310058, China*)

[†]E-mail: shy@zju.edu.cn

Received Jan. 25, 2012; Revision accepted June 7, 2012; Crosschecked July 11, 2012

Abstract: The bending behavior of double-row stabilizing plies is associated with the constructional time delay (CTD), which can be defined as the time interval between the installations of the front stabilizing pile and the rear stabilizing pile. This paper investigates the effect of CTD on the bending moments of double-row stabilizing piles and a method for determining the optimal CTD is proposed. The stabilizing pile is modeled as a cantilever pile embedded in the Winkler elastic foundation. A triangular distributed earth pressure is assumed on the pile segment in the sliding layer. The front stabilizing pile and the rear stabilizing pile are connected by a beam with pinned joints. The analytical solutions of bending moments on the front and the rear stabilizing piles are derived and the accuracy of bending moment solutions is validated by comparing the tensile strain measured from the Hongyan landslide project, Taizhou, Zhejiang, China. It is concluded that CTD has a significant influence on the bending moments of double-row stabilizing piles. An optimal CTD can be obtained when the maximum tensile stress in the front stabilizing pile is equal to that in the rear stabilizing pile, which is 1.4 months for the Hongyan landslide project.

Key words: Subgrade reaction, Landslide, Stabilizing pile, Constructional time delay (CTD), Bending moment
doi:10.1631/jzus.A1200027 **Document code:** A **CLC number:** TU473

1 Introduction

Landslides are a common geological disaster in mountainous construction areas. In order to avoid landslides, slopes usually need to be reinforced. A stabilizing pile is one of the most effective methods used to reinforce the slope. The lateral stiffness of pile groups equals the sum of the lateral stiffness of individual piles (Mokwa, 1999; Mokwa and Duncan, 2003), thus lateral stiffness of double-row piles is larger than that of single-row piles, which leads to a smaller lateral deformation under the same thrust (Leung *et al*., 2003; Won and Kulhawy, 2009). Therefore, double or multi rows of stabilizing piles are used when single-row stabilizing piles cannot provide enough sliding resistance for some large scale landslides (Kang *et al*., 2009). However, safety of a landslide will significantly decrease if boreholes of double-row piles are excavated simultaneously. Therefore, double-row stabilizing piles usually cannot be installed simultaneously in a practical construction process. As a result, the front stabilizing piles are firstly installed to stabilize a potential landslide before the rear ones. In this process, the earth pressure caused by the soil creep on the previous installed stabilizing piles increases, which is influenced by the CTD. In addition, the bending moments on the double-row stabilizing piles will also be different from their design values. Therefore, it is of significance for the civil engineers to study the effect of CTD on the bending behavior of double-row stabilizing plies.

‡ Corresponding author

* Project supported by the National Natural Science Foundation of China (No. 40972187), the Key Innovation Team Support Project of Zhejiang Province (No. 2009R50050), China

Many methods are used to estimate response of laterally loaded piles and pile groups. Numerical methods such as boundary element method (Poulos and Davis, 1980; Hull, 1987; Poulos, 1995; Chen and Poulos, 1997; Xu and Poulos, 2000), finite element and finite difference methods (Bransby and Springman, 1996; Bransby and Springman, 1999) have been widely used in the study of laterally loaded pile and pile groups. Experimental methods (Chen *et al*., 1997; Rollins *et al*., 2005; Ong *et al*., 2009) have been introduced to study the effects of pile interaction (Ashour *et al*., 2004; Chandrasekaran *et al*., 2010; Kim and Yoon, 2011) and pile spacing (Rollins *et al*., 2006; Papadopoulou and Comodromos, 2010) to the response of piles in a group. Although numerical and experimental methods make a lot of contributions to the study of laterally loaded pile response; theoretical study attracted the attention of researchers since the subgrade reaction method was proposed by Hetenyi (1946). Subgrade reaction solutions have been successfully used in predicting response of single laterally loaded piles (Randolph, 1981; Rajani and Morgenstern, 1993; Hsiung, 2003; Cai and Ugai, 2011). However, using theoretical method to study the response of double-row piles acted upon by lateral load has not yet been fully explored.

In this paper, bending moment solutions considering CTD of double-row stabilizing piles are derived based on the subgrade reaction solutions and structural mechanics. Earth pressure, from which the bending moment of the stabilizing pile is derived, is obtained according to displacement history of the front stabilizing pile top. The CTD is considered by dividing bending moment solutions into two stages. The first stage is from the time when the front piles are installed to the time when the rear piles begin working, during this period only the front piles are used to stabilize the landslide. The duration of the first stage equals the CTD. The second stage is the period during which the front and rear stabilizing piles work together. The bending moment solutions are verified using measured strain data of optical fibers installed in the front stabilizing pile of the Hongyan landslide project, which is beside the Zhu-yong expressway (K120+030~K120+200) in Taizhou, Zhejiang, China. Under the action of the same earth pressure, advantages of double-row stabilizing piles are proved by comparing the bending moment distribution and magnitude of single-row stabilizing pile with those of double-row stabilizing pile. An optimal CTD can be obtained when the maximum tensile stress in the front stabilizing pile is equal to that in the rear stabilizing pile, which is 1.4 months for Hongyan landslide project.

2 Governing equations

The following assumptions were introduced to simplify the derivation.

1. Bending behavior of stabilizing pile is linear elastic.

2. Effect of soil between the front and the rear stabilizing piles is neglected. Distribution of the earth pressure on the stabilizing pile is triangular and remains constant as the earth pressure increases.

2.1 Pile segment in sliding layer

The pile segment in the sliding layer is simplified as a cantilever pile, as shown in Fig. 1, M_0 and Q_0 is the bending moment and shear force of stabilizing pile at the depth of sliding surface, respectively; q_0 is the earth pressure at the sliding surface; l_{sl} and l_{st} is the length of pile segments in sliding and stable layer, respectively. Soil resistance behind the piles is ignored since it is just a few meters depth behind the front and rear piles in the present project. Such simplification is conservative for the estimation of bending moment and shear force in piles. Deflection of the cantilever pile is governed by

$$EI\frac{\mathrm{d}^2 y_{\mathrm{cp}}}{\mathrm{d}z_{\mathrm{sl}}^2} = -M_{\mathrm{sl}}(z_{\mathrm{sl}}), \tag{1}$$

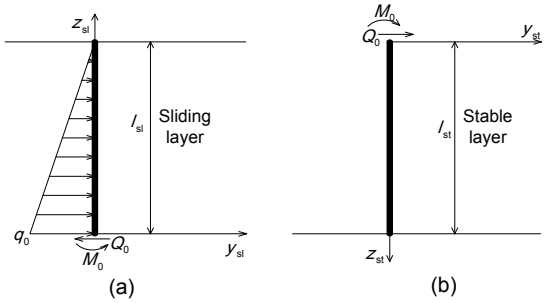

Fig. 1 Coordinate systems and triangular distributed earth pressure

(a) Pile segment in sliding layer; (b) Pile segment in stable layer

where E is the elastic modulus of of the pile, I is the moment of inertia of the pile, y_{cp} is the deflection of the cantilever pile, z_{sl} is the length of pile above the sliding surface, and $M_{sl}(z_{sl})$ is the bending moment of pile segment in the sliding layer.

Eq. (1) can be solved by the second order integration with the boundary condition at z_{sl}=0, rotation angle $\left.\frac{\mathrm{d}y_{cp}}{\mathrm{d}z_{sl}}\right|_{z_{sl}=0}=0$, and deflection $y_{cp}\big|_{z_{sl}=0}=0$. Therefore, by considering the rotation and deflection of the pile at the sliding surface, the deflection of the pile segment in sliding layer y_{sl} can be obtained as

$$y_{sl}=y_0+\varphi_0 z_{sl}+y_{cp}, \tag{2}$$

where y_0 and φ_0 are the deflection and rotation angle of pile at the depth of the sliding surface, respectively, which can be obtained in the next section.

2.2 Pile segment in the stable layer

The pile segment in the stable layer is assumed to be embedded in the Winkler elastic foundation (Fig. 1b). In the Winkler model, the soil medium is considered as a number of independent spring elements which have a stiffness of k_0. The earth pressure q (for unit width) is assumed to be proportional to the deflection of the pile segment in stable layer y_{st}, according to the subgrade reaction theory. The relationship between q and y_{st} can be expressed as

$$q=k_0 b_p y_{st}, \tag{3}$$

where k_0 is the coefficient of subgrade reaction and b_p is the calculated width of the pile (b_p equals the width of cross section b adding 1 m for pile with rectangular cross section).

The effect of axial force in the pile is ignored in the simple theory of the bending of beams (Hsiung, 2003). Thus, the deflection of the pile segment in the stable layer is governed by

$$EI\frac{\mathrm{d}^4 y_{st}}{\mathrm{d}z_{st}^4}+k_0 b_p y_{st}=0, \tag{4}$$

where z_{st} is the length of pile below the sliding surface.

Defining parameter β is equal to $\sqrt[4]{\frac{k_0 b_p}{4EI}}$, Eq. (4) can be derived as

$$\frac{\mathrm{d}^4 y_{st}}{\mathrm{d}z_{st}^4}+4\beta^4 y_{st}=0. \tag{5}$$

The closed-form solution of Eq. (5) has been obtained by Hetenyi (1946). Similar work has been done by Cai and Ugai (2011) who combined the subgrade solutions with required additional resistance in a slope to evaluate the pile response. The deflection of the pile segment in stable layer y_{st} can be expressed as

$$\begin{aligned} y_{st}(z_{st})=&\mathrm{e}^{\beta z_{st}}[A\cos(\beta z_{st})+B\sin(\beta z_{st})]\\ &+\mathrm{e}^{-\beta z_{st}}[C\cos(\beta z_{st})+D\sin(\beta z_{st})], \end{aligned} \tag{6a}$$

where A, B, C, and D are constants.

Rotation φ_{st}, bending moment M_{st}, and shear force Q_{st} of the pile segment in the stable layer can be obtained by taking the first, the second and the third derivatives of displacement field:

$$\begin{aligned} \varphi_{st}(z_{st})=&\beta\mathrm{e}^{\beta z_{st}}[(A+B)\cos(\beta z_{st})-(A-B)\sin(\beta z_{st})]\\ &-\beta\mathrm{e}^{-\beta z_{st}}[(C-D)\cos(\beta z_{st})+(C+D)\sin(\beta z_{st})], \end{aligned} \tag{6b}$$

$$\begin{aligned} M_{st}(z_{st})=&-2EI\beta^2\{\mathrm{e}^{\beta z_{st}}[B\cos(\beta z_{st})-A\sin(\beta z_{st})]\\ &-\mathrm{e}^{-\beta z_{st}}[D\cos(\beta z_{st})-C\sin(\beta z_{st})]\}, \end{aligned} \tag{6c}$$

$$\begin{aligned} Q_{st}(z_{st})=&2EI\beta^3\{\mathrm{e}^{\beta z_{st}}[(A-B)\cos(\beta z_{st})+(A+B)\sin(\beta z_{st})]\\ &-\mathrm{e}^{-\beta z_{st}}[(C+D)\cos(\beta z_{st})-(C-D)\sin(\beta z_{st})]\}. \end{aligned} \tag{6d}$$

In the model presented by Cai and Ugai (2011), both pile segments in sliding and stable layers are in the Winkler elastic foundation. Continuity conditions of the deflection, rotation, bending moment and shear force of the two pile segments at the depth of the sliding surface, combined with the boundary conditions of the bending moment and shear force (both in sliding and stable layers) at the top and bottom of the pile were used to calculate the eight constants in Eq. (6) (four constants in sliding layer and four constants in stable layer). In the proposed model, the pile segment in the sliding layer is assumed to be a cantilever pile. Corresponding continuity conditions used here will be different from those used by Cai

and Ugai (2011). Four constants in Eq. (6) can be determined by assuming that the deflection y_0, rotation φ_0, bending moment M_0, and shear force Q_0 at the depth of sliding surface are already known. Four equation from the continuity conditions of the deflection, rotation, bending moment and shear force of the pile segment in stable layer are used to obtain the constants A, B, C, and D in Eq. (6) as shown in Eq. (7).

$$y_{\mathrm{st}}\big|_{z_{\mathrm{st}}=0}=y_0\Rightarrow A+C=y_0, \tag{7a}$$

$$\varphi_{\mathrm{st}}\big|_{z_{\mathrm{st}}=0}=\varphi_0\Rightarrow (A+B-C+D)\beta=\varphi_0, \tag{7b}$$

$$M_{\mathrm{st}}\big|_{z_{\mathrm{st}}=0}=M_0\Rightarrow -2EI\beta^2(B-D)=M_0, \tag{7c}$$

$$Q_{\mathrm{st}}\big|_{z_{\mathrm{st}}=0}=Q_0\Rightarrow 2EI\beta^3(A-B-C-D)=Q_0. \tag{7d}$$

Solving Eq. (7), the four constants A, B, C, and D can be obtained and Eq. (6) can be expressed as

$$y_{\mathrm{st}}(z_{\mathrm{st}})=y_0\eta_1+\frac{\varphi_0}{\beta}\eta_2+\frac{M_0}{\beta^2EI}\eta_3+\frac{Q_0}{\beta^3EI}\eta_4, \tag{8a}$$

$$\varphi_{\mathrm{st}}(z_{\mathrm{st}})=\beta\left[-4y_0\eta_4+\frac{\varphi_0}{\beta}\eta_1+\frac{M_0}{\beta^2EI}\eta_2+\frac{Q_0}{\beta^3EI}\eta_3\right], \tag{8b}$$

$$M_{\mathrm{st}}(z_{\mathrm{st}})=\beta^2EI\left[-4y_0\eta_3-\frac{4\varphi_0}{\beta}\eta_4+\frac{M_0}{\beta^2EI}\eta_1+\frac{Q_0}{\beta^3EI}\eta_2\right], \tag{8c}$$

$$Q_{\mathrm{st}}(z_{\mathrm{st}})=\beta^3EI\left[-4y_0\eta_2-\frac{4\varphi_0}{\beta}\eta_3-\frac{4M_0}{\beta^2EI}\eta_4+\frac{Q_0}{\beta^3EI}\eta_1\right], \tag{8d}$$

where $\eta_1=\cos(\beta z_{\mathrm{st}})\mathrm{ch}(\beta z_{\mathrm{st}})$, $\eta_2=0.5[\sin(\beta z_{\mathrm{st}})\mathrm{ch}(\beta z_{\mathrm{st}})+\cos(\beta z_{\mathrm{st}})\mathrm{sh}(\beta z_{\mathrm{st}})]$, $\eta_3=0.5\sin(\beta z_{\mathrm{st}})\mathrm{sh}(\beta z_{\mathrm{st}})$, and $\eta_4=0.25[\sin(\beta z_{\mathrm{st}})\mathrm{ch}(\beta z_{\mathrm{st}})-\cos(\beta z_{\mathrm{st}})\mathrm{sh}(\beta z_{\mathrm{st}})]$.

In the present study, the deflection at the bottom of the pile segment in stable layer could be constrained by the wall of the pile hole, but rotation is free to develop. Therefore, a pinned joint mechanism is assumed. Thus, the bending moment and deflection are assumed to be zero. In Eq. (8), M_0 and Q_0 is equal to the bending moment and shear force of the pile segment in sliding layer at the depth of sliding surface, respectively. y_0 and φ_0 can be obtained from the boundary condition that both the bending moment and deflection at the bottom of the pile equal zero (pinned joint), which can be given by

$$y_0=\frac{M_0}{\beta^2EI}\frac{4\eta_3\eta_4+\eta_1\eta_2}{4\eta_2\eta_3-4\eta_1\eta_4}+\frac{Q_0}{\beta^3EI}\frac{4\eta_4^2+\eta_2^2}{4\eta_2\eta_3-4\eta_1\eta_4}\bigg|_{z_{\mathrm{st}}=l_{\mathrm{st}}}, \tag{9a}$$

$$\varphi_0=-\frac{M_0}{\beta EI}\frac{\eta_1^2+4\eta_3^2}{4\eta_2\eta_3-4\eta_1\eta_4}-\frac{Q_0}{\beta^2EI}\frac{4\eta_3\eta_4+\eta_1\eta_2}{4\eta_2\eta_3-4\eta_1\eta_4}\bigg|_{z_{\mathrm{st}}=l_{\mathrm{st}}}. \tag{9b}$$

Substituting M_0, Q_0, and Eq. (9) into Eq. (8), the deflection, rotation, bending moment, and shear force of pile segment in stable layer can be obtained.

3 Bending moment calculation of double-row piles

Based on previous analyses, it can be found that the bending moment of the pile segment in the stable layer is a function of M_0 and Q_0, which is equal to the bending moment and shear force of the pile segment in the sliding layer at the depth of the sliding surface. For a pile under triangular distributed earth pressure, the bending moment of the pile segment in the stable layer is a function of q_0, which is the magnitude of earth pressure (for unit width) caused by creep deformation of the slope at the depth of the sliding surface. The bending moments can be theoretically obtained from the deflection curve of the pile according to the governing Eqs. (1) and (5). However, it is more convenient and economic to measure the head displacement than measure the deflection of the whole pile. Based on the assumption that pile behavior is linear elastic, pile head displacement y_{top} can be used to calculate the bending moment by establishing a relationship of y_{top} and q_0. Consequently, earth pressure history $q_0(t)$ can be obtained according to the monitored head displacement history $y_{\mathrm{top}}(t)$. For double-row stabilizing piles it is assumed that the front pile starts working from the time when it is installed, and rear pile starts working at the time of $t=t_{\mathrm{D}}$ with earth pressure history $q_0(t)$, where t_{D} is the time when rear pile and beam were installed. Thus, the bending moment calculation of double-row piles can be divided into two stages.

3.1 Stage one: the front pile working alone ($t\leq t_{\mathrm{D}}$)

At the stage when the front pile works alone (Fig. 2), the bending moment and shear force of the

pile segment at a point z_1, the length of the front pile above sliding surface, can be expressed as

$$M(z_1,t)=\frac{bq_0(t)(l_1-z_1)^3}{6l_1}, \tag{10a}$$

$$Q(z_1,t)=\frac{bq_0(t)(l_1-z_1)^2}{2l_1}, \tag{10b}$$

where b is the width of pile cross section, l_1 is the length of front pile segment in the sliding layer.

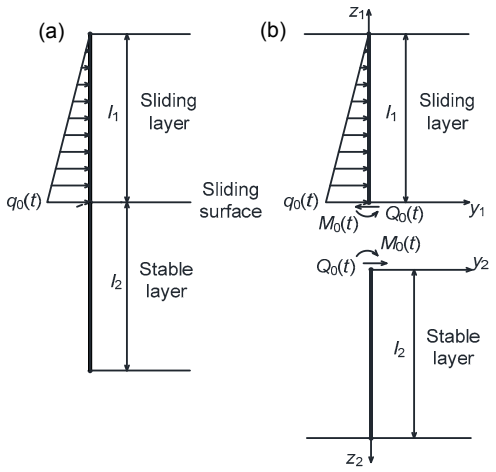

Fig. 2 Models of front stabilizing pile at stage one
(a) Schematic model of front stabilizing pile; (b) Mechanical model of front stabilizing pile

The front pile head deflection $y_{\text{top}}(t)$ can be expressed as

$$y_{\text{top}}(t)=y_0-\varphi_0 l_1+\frac{bq_0(t)l_1^4}{30EI_1}, \tag{11}$$

where I_1 is the moment of inertia of the front pile, y_0 is the displacement at the depth of the sliding surface, and φ_0 is the rotation at the depth of the sliding surface.

The third term at the right side of Eq. (11) is the head deflection of the front pile as a cantilever pile under the action of triangular distributed earth pressure. Note that the directions of z_1 and z_2 are opposite to each other (z_2 is the length of the front pile below the sliding surface), thus there is a minus sign before φ_0 in Eq. (11). y_0 and φ_0 are calculated according to Eq. (9) in which the moment of inertia and length of the pile segment in the stable layer should be replaced by I_1 and l_2 (the length of front pile segment in stable layer). The bending moment and shear force at the depth of the sliding surface can be obtained from Eq. (10):

$$M_0(t)=M(z_1,t)\big|_{z_1=0}=\frac{bq_0(t)l_1^2}{6}, \tag{12a}$$

$$Q_0(t)=Q(z_1,t)\big|_{z_1=0}=\frac{bq_0(t)l_1}{2}. \tag{12b}$$

Substituting Eqs. (9) and (12) into Eq. (11) yields

$$q_0(t)=\frac{y_{\text{top}}(t)}{\delta_{y_{\text{top}}q_0}}, \tag{13}$$

where $\delta_{y_{\text{top}}q_0}=b\left(\frac{l_1^2}{6\beta_1^2EI_1}\lambda_1+\frac{l_1}{2\beta_1^3EI_1}\lambda_2+\frac{l_1^3}{6\beta_1EI_1}\lambda_3+\frac{l_1^2}{2\beta_1^2EI_1}\lambda_4+\frac{l_1^4}{30EI_1}\right)$, $\lambda_1=\lambda_4=\left.\frac{4\eta_3\eta_4+\eta_1\eta_2}{4\eta_2\eta_3-4\eta_1\eta_4}\right|_{z_2=l_2}$, $\lambda_2=\left.\frac{4\eta_4^2+\eta_2^2}{4\eta_2\eta_3-4\eta_1\eta_4}\right|_{z_2=l_2}$, $\lambda_3=\left.\frac{\eta_1^2+4\eta_3^2}{4\eta_2\eta_3-4\eta_1\eta_4}\right|_{z_2=l_2}$, $\beta_1=\sqrt[4]{\frac{k_0b_{\text{p}}}{4EI_1}}$.

Substituting Eq. (13) into Eq. (10a) the bending moment of the front pile segment in the sliding layer is calculated from head deflection, and can be expressed as

$$M(z_1,t)=\frac{by_{\text{top}}(t)(l_1-z_1)^3}{6\delta_{y_{\text{top}}q_0}l_1}. \tag{14a}$$

Substituting Eqs. (9), (12) and (13) into Eq. (8c) the bending moment of the front pile segment in the stable layer calculated from the head displacement can be expressed as

$$M(z_2,t)=\frac{by_{\text{top}}(t)}{\delta_{y_{\text{top}}q_0}}\left[-\left(\frac{2l_1^2}{3}\lambda_1+\frac{2l_1}{\beta_1}\lambda_2\right)\eta_3+\left(\frac{2l_1^2}{3}\lambda_3+\frac{2l_1}{\beta_1}\lambda_4\right)\eta_4+\frac{l_1^2}{6}\eta_1+\frac{l_1}{2\beta_1}\eta_2\right]. \tag{14b}$$

3.2 Stage two: double-row stabilizing piles working together ($t\geq t_{\text{D}}$)

If creep deformation of the slope continues developing after the installation of a rear stabilizing pile

and the connecting beam, the axial force $N(t)$ will develop in the connecting beam and act on points 1 and 2 as shown in Fig. 3. Part of the increment of earth pressure $q_0(t)-q_0(t_D)$ caused by the continuous creeping is transferred from the front pile to the rear pile by the connecting beam (in the condition that the effect of soil between front and rear piles is ignored). Pinned joints are assumed at the points where the front and rear piles connect with the beam. The bending moment of the front pile at stage two can be divided into two parts by t_D. The first part is the magnitude of the bending moment at the end of stage one $M(z, t_D)$. The second part is the increment of bending moment caused by the increment of earth pressure $M(z, t-t_D)$. Increments of bending moment and shear force of the front pile can be expressed as

$$M(z_1,t-t_D)=\begin{cases}\dfrac{b[q_0(t)-q_0(t_D)](l_1-z_1)^3}{6l_1}\\ \quad -N(t)(l_3-z_1),\ 0\le z_1\le l_3,\\ \dfrac{b\left[q_0(t)-q_0(t_D)\right](l_1-z_1)^3}{6l_1},\ l_3\le z_1\le l_1,\end{cases} \tag{15a}$$

$$Q(z_1,t-t_D)=\begin{cases}\dfrac{b[q_0(t)-q_0(t_D)](l_1-z_1)^2}{2l_1}\\ \quad -N(t),\ 0\le z_1\le l_3,\\ \dfrac{b[q_0(t)-q_0(t_D)](l_1-z_1)^2}{2l_1},\quad l_3\le z_1\le l_1,\end{cases} \tag{15b}$$

where l_3 is the length of the rear pile segment in the sliding layer.

Increments of bending moment and shear force of the front pile at the depth of the sliding surface can be obtained according to Eq. (15):

$$\begin{aligned}M_0(t-t_D)&=M(z_1,t-t_D)\big|_{z_1=0}\\&=\frac{b[q_0(t)-q_0(t_D)]l_1^2}{6}-N(t)l_3,\end{aligned} \tag{16a}$$

$$\begin{aligned}Q_0(t-t_D)&=Q(z_1,t-t_D)\big|_{z_1=0}\\&=\frac{b[q_0(t)-q_0(t_D)]l_1}{2}-N(t).\end{aligned} \tag{16b}$$

Increments of head deflection of the front pile can be expressed as

$$\begin{aligned}y_{top}(t)-y_{top}(t_D)=y_0-\varphi_0 l_1+\frac{b[q_0(t)-q_0(t_D)]l_1^4}{30EI_1}\\ -\frac{N(t)l_3^2}{6EI_1}(3l_1-l_3).\end{aligned} \tag{17}$$

The fourth term at the right side of Eq. (17) is the head deflection of the front pile as a cantilever pile under the action of $N(t)$ coming from connecting beam. y_0 and φ_0 are also the increments of deflection and rotation at the sliding surface caused by the increment of earth pressure $q_0(t)-q_0(t_D)$. In Eq. (16), the relationship between $N(t)$ and $q_0(t)$ should be firstly determined, in order to establish the relationship

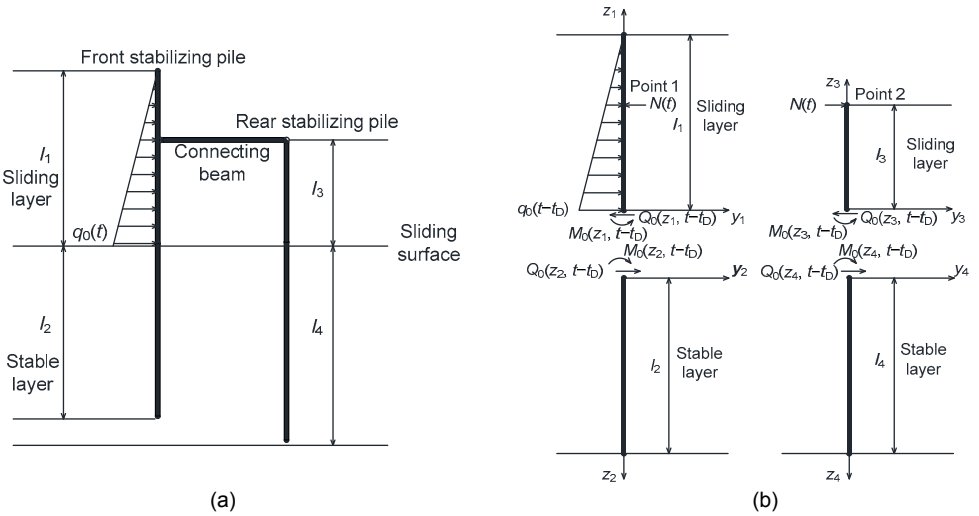

Fig. 3 Models of double-row stabilizing piles at stage two
(a) Schematic model of double-row stabilizing piles; (b) Mechanical model of double-row stabilizing piles

between $y_{top}(t)-y_{top}(t_D)$ and $q_0(t)-q_0(t_D)$. Deflections y_1 and y_2 at the points 1 and 2 where the front and rear piles connect with the beam (Fig. 3b) are given by

$$y_1(t)=b[q_0(t)-q_0(t_D)]\left[\frac{l_1^2\lambda_1}{6\beta_1^2EI_1}+\frac{l_1\lambda_2}{2\beta_1^3EI_1}+\frac{l_1^2l_3\lambda_3}{6\beta_1EI_1}+\frac{l_1l_3\lambda_4}{2\beta_1^2EI_1}+\frac{(l_1-l_3)^5+5l_1^4l_3-l_1^5}{120EI_1l_1}\right]-N(t)\left(\frac{l_3^3}{3EI_1}+\frac{l_3\lambda_1}{\beta_1^2EI_1}+\frac{\lambda_2}{\beta_1^3EI_1}+\frac{l_3^2\lambda_3}{\beta_1EI_1}+\frac{l_3\lambda_4}{\beta_1^2EI_1}\right), \tag{18a}$$

$$y_2(t)=N(t)\left(\frac{l_3\lambda_1'}{\beta_2^2EI_2}+\frac{\lambda_2'}{\beta_2^3EI_2}+\frac{l_3^2\lambda_3'}{\beta_2EI_2}+\frac{l_3\lambda_4'}{\beta_2^2EI_2}+\frac{l_3^3}{3EI_2}\right), \tag{18b}$$

where λ_1', λ_2', λ_3', and λ_4' have the same formulas as λ_1, λ_2, λ_3 and λ_4 but with a different moment of inertia and length of pile segment in the stable layer. In λ_1', λ_2', λ_3', and λ_4', I (in λ_1, λ_2, λ_3 and λ_4) is replaced by moment inertia of the rear pile I_2, and l_{st} is replaced by the length of rear pile segment in the stable layer l_4.

Continuity conditions of deflections at the two ends of the connecting beam are used which is $y_1=y_2$. As a result, $N(t)$ can be expressed as

$$N(t)=\alpha b[q_0(t)-q_0(t_D)], \tag{19}$$

where

$$\alpha=\left[\frac{l_1^2}{6\beta_1^2EI_1}\lambda_1+\frac{l_1}{2\beta_1^3EI_1}\lambda_2+\frac{l_1^2l_3}{6\beta_1EI_1}\lambda_3+\frac{l_1l_3}{2\beta_1^2EI_1}\lambda_4+\frac{(l_1-l_3)^5+5l_1^4l_3-l_1^5}{120EI_1l_1}\right]\Bigg/\left[\frac{l_3}{\beta_2^2EI_2}\lambda_1'+\frac{1}{\beta_2^3EI_2}\lambda_2'+\frac{l_3^2}{\beta_2EI_2}\lambda_3'+\frac{l_3}{\beta_2^2EI_2}\lambda_4'+\frac{l_3^3}{3EI_2}+\frac{l_3}{\beta_1^2EI_1}\lambda_1+\frac{1}{\beta_1^3EI_1}\lambda_2+\frac{l_3^2}{\beta_1EI_1}\lambda_3+\frac{l_3}{\beta_1^2EI_1}\lambda_4+\frac{l_3^3}{3EI_1}\right].$$

Substituting Eqs. (9), (16) and (19) into Eq. (17) yields the relationships between $y_{top}(t)-y_{top}(t_D)$ and $q_0(t)-q_0(t_D)$ at stage two, which is expressed as

$$q_0(t)-q_0(t_D)=\frac{y_{top}(t)-y_{top}(t_D)}{\delta'_{y_{top}q_0}}, \tag{20}$$

where

$$\delta'_{y_{top}q_0}=b\left(\frac{l_1^2}{6}-\alpha l_3\right)\left(\frac{\lambda_1}{\beta_1^2EI_1}+\frac{\lambda_3l_1}{\beta_1EI_1}\right)+\left(\frac{l_1}{2}-\alpha\right)\left(\frac{\lambda_2}{\beta_1^3EI_1}+\frac{\lambda_4l_1}{\beta_1^2EI_1}\right)+\frac{l_1^4-5\alpha l_3^2(3l_1-l_3)}{30EI_1}.$$

Substituting Eq. (20) into Eq. (16a) the bending moment of the front pile segment in sliding layer in the displacement form at stage two can be obtained:

$$M(z_1,t)=\begin{cases}M(z_1,t_D)+\dfrac{b[y_{top}(t)-y_{top}(t_D)]}{\delta'_{y_{top}q_0}}\left[\dfrac{(l_1-z_1)^3}{6l_1}-\alpha(l_3-z_1)\right], & 0\le z_1\le l_3,\\ M(z_1,t_D)+\dfrac{b[y_{top}(t)-y_{top}(t_D)](l_1-z_1)^3}{6\delta'_{y_{top}q_0}l_1}, & l_3<z_1\le l_1,\end{cases} \tag{21a}$$

where $M(z_1, t_D)$ is obtained according to Eq. (14a) when t equals t_D.

Substituting Eqs. (9), (16) and (20) into Eq. (8c), the bending moment of the front pile segment in the stable layer in the displacement form at stage two can be obtained:

$$M(z_2,t)=M(z_2,t_D)+\frac{b[y_{top}(t)-y_{top}(t_D)]}{\delta'_{y_{top}q_0}}\left[\left(\frac{l_1^2}{6}-\alpha l_3\right)\cdot(-4\lambda_1\eta_3+4\lambda_3\eta_4+\eta_1)+\left(\frac{l_1}{2}-\alpha\right)\left(\frac{-4\lambda_2\eta_3+4\lambda_4\eta_4+\eta_2}{\beta_1}\right)\right], \tag{21b}$$

where $M(z_2, t_D)$ is obtained according to Eq. (14b) when t equals t_D.

The bending moment and shear force of the rear pile segment in the sliding layer are

$$M(z_3,t)=N(t)(l_3-z_3), \tag{22a}$$

$$Q(z_3,t)=N(t), \tag{22b}$$

where z_3 is the length of the rear pile above the sliding surface.

The bending moment and shear force of the rear

pile in the sliding layer at the depth of the sliding surface can be obtained according to Eq. (22):

$$M_0(t)=M_0(z_3,t)\big|_{z_3=0}=N(t)l_3, \tag{23a}$$

$$Q_0(t)=Q_0(z_3,t)\big|_{z_3=0}=N(t). \tag{23b}$$

Substituting Eqs. (19) and (20) into Eq. (22) the bending moment of rear pile segments in the sliding layer in the displacement form can be expressed as

$$\begin{aligned}M(z_3,t)&=\alpha b[q_0(t)-q_0(t_D)](l_3-z_3)\\&=\frac{\alpha b[y_{\text{top}}(t)-y_{\text{top}}(t_D)](l_3-z_3)}{\delta'_{y_{\text{top}}q_0}}.\end{aligned} \tag{24a}$$

Substituting Eqs. (9), (19), (20) and (23) into Eq. (8c) the bending moment of rear pile segments in the stable layer in the displacement form can be expressed as

$$\begin{aligned}M(z_4,t)=&\frac{\alpha b[y_{\text{top}}(t)-y_{\text{top}}(t_D)]}{\delta'_{y_{\text{top}}q_0}}[l_3(-4\lambda_1'\eta_3'+4\lambda_3'\eta_4'+\eta_1')\\&+(-4\lambda_2'\eta_3'+4\lambda_4'\eta_4'+\eta_2')/\beta_2],\end{aligned} \tag{24b}$$

where $\eta_1'=\cos(\beta_2 z_4)\text{ch}(\beta_2 z_4)$, $\eta_2'=0.5[\sin(\beta_2 z_4)\text{ch}(\beta_2 z_4)+\cos(\beta_2 z_4)\text{sh}(\beta_2 z_4)]$, $\eta_3'=0.5\sin(\beta_2 z_4)\text{sh}(\beta_2 z_4)$, $\eta_4'=0.25[\sin(\beta_2 z_4)\text{ch}(\beta_2 z_4)-\cos(\beta_2 z_4)\text{sh}(\beta_2 z_4)]$, and z_4 is the length of the rear pile below the sliding surface.

4 Application and results

Hongyan landslide (Fig. 4) was triggered by the excavation of the slope toe. The average width, length, area and volume of the landslide were approximately 80 m, 75 m, 5700 m^2 and 4.56×10^5 m^3, respectively. The plan view of the landslide is shown in Fig. 5. The landslide was predominantly controlled using the front stabilizing piles. 5 months later rear stabilizing piles were installed as remediation, since surface displacements of the slope still developed very fast after installation of the front stabilizing piles. Double-row stabilizing piles are shown in Fig. 6. The cross section dimensions of the front and rear stabilizing piles were 2 m×3 m and 2 m×3.5 m, respectively. C30 concrete was used to build the piles. The coefficient of subgrade reaction of bedrock equals 3.5×10^4 kN/m^3. Parameters used to calculate the bending moments of double-row stabilizing piles are shown in Table 1.

Fig. 4 Hongyan landslide

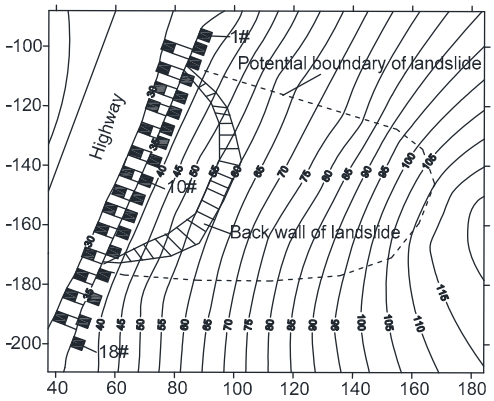

Fig. 5 Plan view of Hongyan landslide (unit: m)

Fig. 6 Double-row stabilizing piles in Hongyan landslide

Table 1 Relevent parameters used in the calculation of bending moments

Parameter	Value	Parameter	Value
EI_1 (N·m^2)	1.35×10^{11}	l_3 (m)	17
EI_2 (N·m^2)	2.14×10^{11}	l_4 (m)	12.5
β_1 (m^{-1})	0.1181	$\delta_{y_{\text{top}}q_0}$ (m^3/N)	7.45×10^{-7}
β_2 (m^{-1})	0.1052	α (m)	3.77
l_1 (m)	24	$\delta'_{y_{\text{top}}q_0}$ (m^3/N)	2.96×10^{-7}
l_2 (m)	11		

Fig. 7 shows the head deflection history of the front stabilizing pile measured by electronic total station. The landslide had been in creeping stage when the front piles were being installed; soil in the sliding layer was moving slowly downslope. After installation of the front piles, earth pressure will act on front piles due to the relative displacement between soil and piles. As a result, bending moment and shear force, which are related to the deflection of piles, will develop. The curve in Fig. 7 can be divided into three stages, according to displacement rate: 1. From Dec. 20, 2009 to Feb. 11, 2010, the head displacement rate was the largest in the three stages. This was attributed to the fact that 8 m depth of soil behind the front stabilizing pile was removed in order to build a platform for the installation of the rear stabilizing pile, and boreholes of rear stabilizing piles were excavated during this period. This construction activity resulted in the decrease of soil resistance behind the front stabilizing pile. 2. From Feb. 11, 2010 to May 22, 2010, the rate of head displacement of front stabilizing pile decreased. The explanation was that earth pressure gradually acted on the piles as the relative displacement between soil and piles developed (caused by soil creep deformation around the pile), which led to a gradual increase of the bending moment and shear force in piles. As a result, resistance provided by the bending moment and shear force of the pile gradually increased. The data of the inclinometer illustrated that the lateral deformation of the soil between the front and rear stabilizing piles is very small, which meant the sliding force was not transmitted from the front stabilizing pile to the rear stabilizing pile through the soil in this stage. The rear stabilizing pile was just for emergency capacity, and the front stabilizing pile was considered to be working alone in this stage. 3. From May 22, 2010 to Oct. 19, 2010, the connecting beam was installed. The double-row stabilizing piles started working together, and the thrust was transmitted from the front stabilizing pile to rear stabilizing pile by the beam. The rate of the head displacement decreased since lateral stiffness of the double-row pile was larger than the single ones. The head displacement of the front stabilizing pile tended to be a constant value.

Bending moments of double-row stabilizing piles, calculated based on the presented model, are shown in Fig. 8.

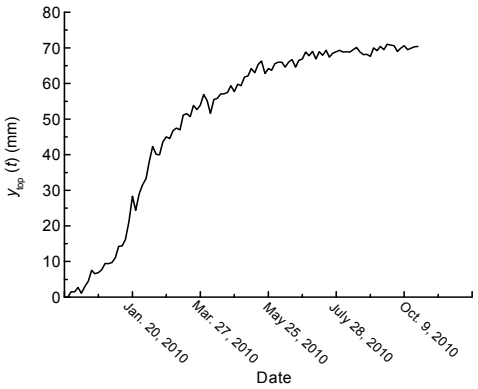

Fig. 7 Curve of the head displacement of the front stabilizing pile

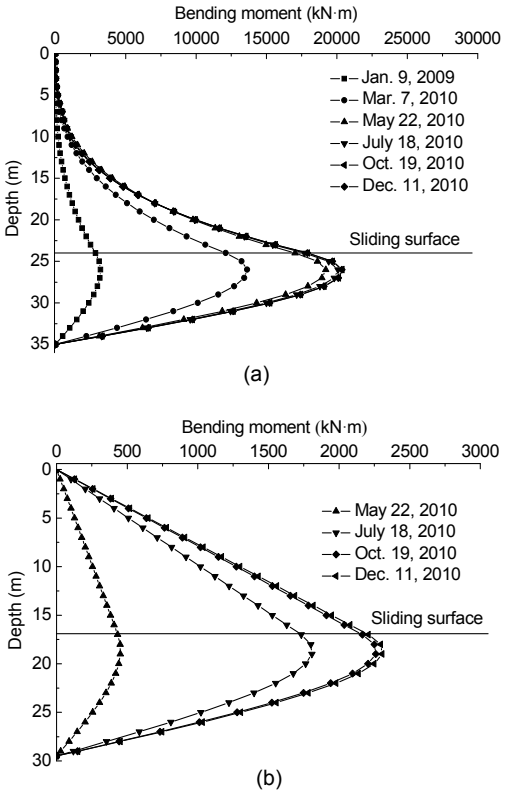

Fig. 8 Bending moments of front stabilizing pile (a) and rear stabilizing pile (b) at different dates

Single-row concrete (Esu and D'Elia, 1974) and steel (Fukumoto, 1976) piles were used to stabilize landslides. Piles in the two cases were instrumented to measure their bending behaviors, and parameters are shown in Table 2. These two cases have been used by Cai and Ugai (2011) to verify accuracy of the model proposed by them.

Fig. 9 shows the bendimg moments calculated using the models proposed in this study and by Cai

Table 2 Parameters in the cases reported by Esu and D'Elia (1974) and Fukumoto (1976)

Case	EI (N·m^2)	β (m^{-1})	Pile length in sliding layer (m)	Pile length in stable layer (m)	Coefficient of subgrade reaction (MPa)	q_0 (kN/m)
Esu and D'Elia (1974)	1.7×10^7	0.583	7.5	22.5	8	78.93
Fukumoto (1976)	3.8×10^8	0.269	4	6	8	125

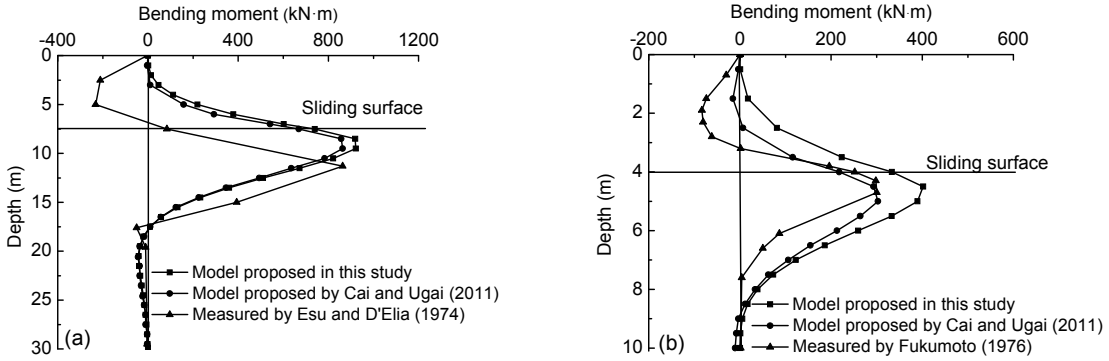

Fig. 9 Comparison of bending moments based on present model, Cai and Ugai (2011)'s model and field measurement by (a) Esu and D'Elia (1974); (b) Fukumoto (1976)

and Ugai (2011) and measured by Esu and D'Elia (1974) and Fukumoto (1976). Bending moment distribution of the model presented in this study is similar to that proposed by Cai and Ugai (2011); however, larger magnitudes of bending moment are predicted by the developed model than that predicted by Cai and Ugai (2011). The reason is that in the sliding layer, soil resistance behind the pile is neglected in the developed model but considered in the model proposed by Cai and Ugai (2011). Because the soil behined the front and rear stabilizing piles was removed in Hongyan landslide, it would be more appropriate using the developed model than the Cai-Ugai model to predict bending moments of piles in Hongyan landslide.

Optical fiber was installed in the tension side of No. 10 front stabilizing pile, as shown in Fig. 10. Strain data were measured by Brillouin Optical Time Domain Reflector (BOTDR). In order to verify the accuracy of the bending moment solutions presented in this study, the strains calculated according to bending moment in Eqs. (14) and (21) are also compared with the measured strains, as shown in Fig. 11. It is assumed that the pile section behaves as a rigid plane and it remains perpendicular to the pile axis after deflecting, but stretching cannot occur. Strain distribution over the pile section is shown in Fig. 10. Consequently, the strain calculated from bending

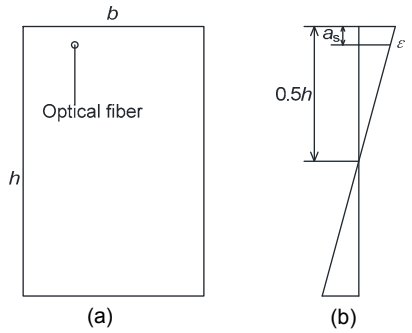

Fig. 10 Position of optical fiber (a) and strain distribution over pile section (b)

moment solutions at the same position with optical fiber can be obtained by

$$\varepsilon = \frac{M(0.5h - a_s)}{EI}, \tag{25}$$

where M is the bending moment calculated according to Eqs. (14) and (21), h is the height of the pile cross section, and a_s is the distance between optical fibers and edge of the tension side of the pile, here a_s equals 10 cm.

There are two significant discrepancies in Fig. 11. One is from pile head to 25 m, the other is below 33 m. The front pile from pile head to 10 m is exposed to the environment. The strain data measured by optical fibers are significantly influenced by

temperature changing in the environment. As a result, there are rather large strains at the head of pile which is unreasonable for a free-head pile.

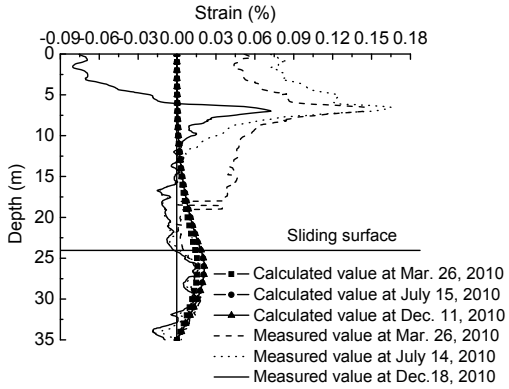

Fig. 11 Comparison between measured and calculated strains

Compressive strains are measured from 14 m to 23 m, where the largest discrepancies occur. This is because in the proposed model the sliding layer is assumed to be homogeneous, but in Hongyan landslide project there are several soil layers distributed in the sliding layer, which leads to a complicated distribution of earth pressure (it is not an ideal triangular distributed earth pressure). Surface of the landslide and soils over 7 m between piles were concreted and anchored, resulting in a smaller deformation in the upper part than that in the deeper part of the sliding layer; reverse bending will develop in the deeper part of the sliding layer. If the earth pressure acting on the pile segment in the sliding layer can be measured, this problem will be solved (Smethurst and Powrie, 2007).

The measured and calculated strains fit well over the pile segment in the stable layer where engineers pay a lot of attention in pile design. But there is a saddle distribution from 26 m to 30 m. It seems that there are two cracks developing at depths of 26 m and 30 m. As a result, the strain between cracks will decrease (Clark and Richards, 2005; de Sousa Coutinho, 2006). Small compressive strains were measured bellow 33 m which is caused by self-weight and shrinkage of concrete.

5 Discussion

Earth pressure history at the sliding surface $q_0(t)$ can be obtained from head displacement history in Fig. 7 by back analysis according to Eqs. (13) and (20), as shown in Fig. 12. Consequently, the bending moment of the stabilizing pile can be obtained according to Eqs. (13) and (14) if the landslide is stabilized just using the front stabilizing piles. Bending moment comparison between single- and double-row stabilizing piles is shown in Fig. 13. It can be observed that when the landslide is stabilized just using the front piles, bending moments are larger than that in the front pile on the condition that the landslide is stabilized using double-row piles. Increment of bending moment in single-row piles is also larger than that in the front pile of the double-row piles. These phenomena can be explained by Eqs. (13) and (20), in which $\delta_{y_{\text{top}}q_0} / \delta'_{y_{\text{top}}q_0}$ is equal to 2.52 (Table 1). It means that under the action of the same increment of earth pressure, the increment of bending moment in single-row piles is 2.52 times larger than that in the front pile of double-row piles (under the linear elastic

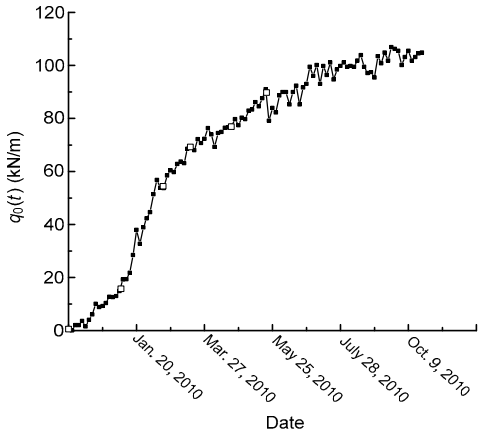

Fig. 12 Earth pressure history at the sliding surface

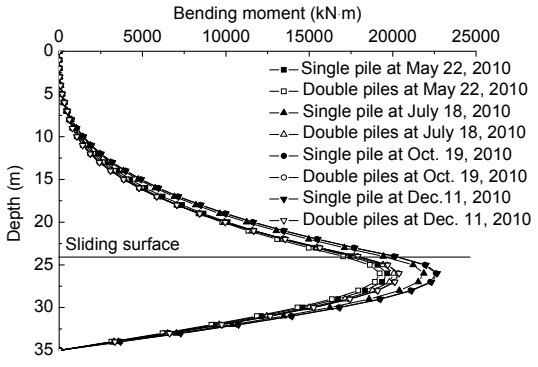

Fig. 13 Comparison of bending moments of front stabilizing pile between the condition that the front pile working alone and the condtion that front and rear piles working together

assumption increment of bending moment being proportional to the increment of head displacement). The lateral stiffness of double-row piles is 2.52 times larger than that of front row of piles.

CTD of double-row stabilizing piles is 5 months for Hongyan landslide project (the front piles were installed on Dec. 20, 2009 and the rear piles and connecting beam were installed on May 22, 2010). When CTD is equal to 0, 1, 2, 3 and 4 months, which means that the rear stabilizing piles start working at Dec. 22, 2009, Jan. 20, 2010, Feb. 20, 2010, Mar. 19, 2010 and Apr. 20, 2010, respectively, bending moments of the front and rear piles at Dec. 11, 2010 are shown in Figs. 14a and 14b.

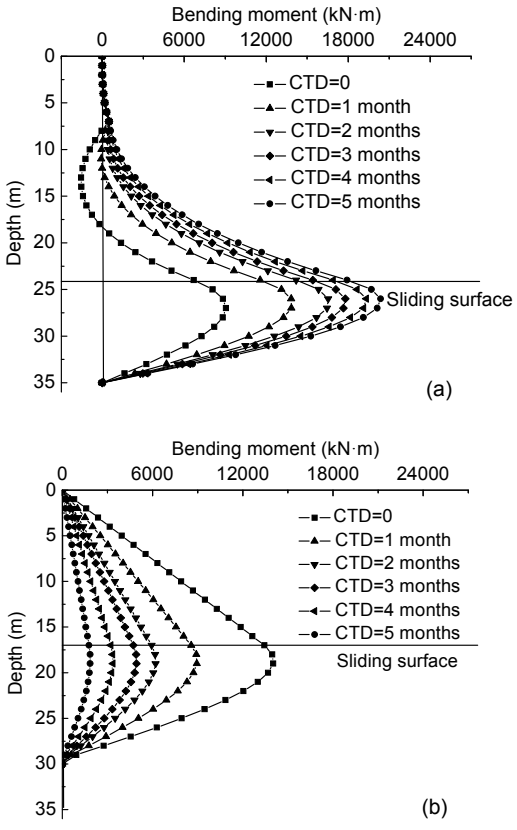

Fig. 14 Bending moments of front stabilizing pile (a) and rear stabilizing pile (b) at Dec. 11, 2010 with different CTDs

Fig. 14a shows that CTD has less influence on the bending moment of the front stabilizing pile above the point where the beam connects with the front pile. However, bending moment significantly increases as CTD increases below the point, where the beam connects with front pile and negative bending moment develops in the pile segment in the sliding layer when CTD is between 0 and 1 month. Fig. 14b shows that bending moment of the rear stabilizing pile significantly decreases as CTD increases, which is different from that in the front pile as shown in Fig. 14a. In order to make full use of pile materials, an optimal CTD can be obtained when $\sigma_{\mathrm{rmax}}=\sigma_{\mathrm{fmax}}$ is taken as the optimization goal (where σ_{rmax} and σ_{fmax} are the maximum tensile stresses of rear and front stabilizing piles, respectively). The maximum tensile stresses of rear and front stabilizing piles are given by

$$\sigma_{\mathrm{rmax}}=\frac{0.5h_{\mathrm{r}}M_{\mathrm{rmax}}}{I_{\mathrm{r}}}, \tag{26a}$$

$$\sigma_{\mathrm{fmax}}=\frac{0.5h_{\mathrm{f}}M_{\mathrm{fmax}}}{I_{\mathrm{f}}}, \tag{26b}$$

where h_{r} and h_{f} is the height of rear and front pile sections, respectively; I_{r} and I_{f} is the second moment of area of rear and front pile sections, respectively; and M_{rmax} and M_{fmax} is the maximum bending moment of rear and front piles, respectively.

Ratios of maximum tensile stresses of rear to front stabilizing pile, when CTD is equal to 0, 1 month, 2 months, 3 months, 4 months, and 5 months are shown in Fig. 15. It can be seen that the optimal CTD in the Hongyan landslide project is about 1.4 months, which is much shorter than practical CTD (5 months). When CTD is equal to 5 months the maximum tensile stress in rear stabilizing pile is only one fifth of that in front stabilizing pile. Part of the construction cost is wasted since the materials are not fully used.

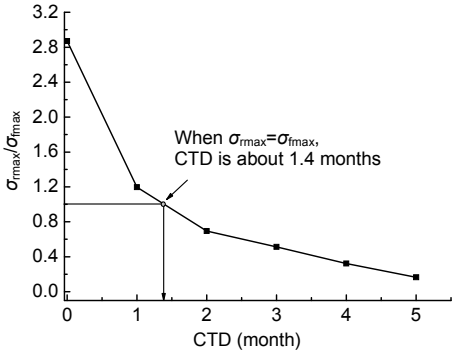

Fig. 15 Ratios of maximum tensile stress of rear to front stabilizing piles with different CTDs

6 Conclusions

Bending moments of double-row stabilizing piles considering CTDs based on subgrade reaction solutions and structural mechanics are addressed in this paper. The solutions were verified by comparing strain data measured by optical fibers. The results show that the present method is accurate in the stable layer where the maximum bending moments develop in stabilizing piles. Comparison of the bending moments between single- and double-row stabilizing piles shows that deflection of double-row stabilizing piles is smaller than that of single-row pile under the action of the same earth pressure. CTD has a significant effect on the distribution and magnitude of bending moments of the front and the rear stabilizing piles. For full use of the materials of stabilizing pile consideration, CTD in Hongyan landslide project is recommended to be 1.4 months.

Acknowledgements

The authors wish to thank Prof. Leonardo CASCINI and his colleagues, the University of Salerno, Italy, Dr. Yong-li LIU, the Wuhan Institute of Rock and Soil Mechanics, Chinese Academy of Sciences, and Dr. Li-feng FAN, the Nanyang Technological University, Singapore, for their advice and kindly help.

References

Ashour, M., Pilling, P., Norris, G., 2004. Lateral behavior of pile groups in layered soils. *Journal of Geotechnical and Geoenvironmental Engineering*, **130**(6):580-592. [doi:10.1061/(ASCE)1090-0241(2004)130:6(580)]

Bransby, M.F., Springman, S.M., 1996. 3-D finite element modelling of pile groups adjacent to surcharge loads. *Computers and Geotechnics*, **19**(4):301-324. [doi:10.1016/0266-352X(95)00001-Q]

Bransby, M.F., Springman, S.M., 1999. Selection of load-transfer functions for passive lateral loading of pile groups. *Computers and Geotechnics*, **24**(3):155-184. [doi:10.1016/S0266-352X(99)00006-3]

Cai, F., Ugai, K., 2011. A subgrade reaction solution for piles to stabilise landslides. *Geotechnique*, **61**(2):143-151. [doi:10.1680/geot.9.P.026]

Chandrasekaran, S.S., Boominathan, A., Dodagoudar, G.R., 2010. Group interaction effects on laterally loaded piles in clay. *Journal of Geotechnical and Geoenvironmental Engineering*, **136**(4):573-582. [doi:10.1061/(ASCE)GT.1943-5606.0000245]

Chen, L.T., Poulos, H.G., 1997. Piles subjected to lateral soil movements. *Journal of Geotechnical and Geoenvironmental Engineering*, **123**(9):802-811. [doi:10.1061/(ASCE)1090-0241(1997)123:9(802)]

Chen, L.T., Poulos, H.G., Hull, T.S., 1997. Model tests on pile groups subjected to lateral soil movement. *Soils and Foundations*, **37**(1):1-12. [doi:10.3208/sandf.37.1]

Clark, J., Richards, D.J., 2005. Measurement of Bending Moment in Concrete. Proceeding of the 16th International Conference Soil Mechanics and Geotechnical Engineering, Osaka, **2**:1027-1030.

de Sousa Coutinho, A.G.F., 2006. Data reduction of horizontal load full-scale tests on bored concrete piles and pile groups. *Journal of Geotechnical and Geoenvironmental Engineering*, **132**(6):752-769. [doi:10.1061/(ASCE)1090-0241(2006)132:6(752)]

Esu, F., D'Elia, B., 1974. Interazione terreno-struttura in un palo sollectato dauna frana tipo colata. *Rivsita Italiana di Geotechica*, **8**(1):27-38 (in Italian).

Fukumoto, Y., 1976. The behaviour of piles for preventing landslide. *Soils and Foundations*, **16**(2):91-103 (in Japanese). [doi:10.3208/sandf1972.16.2_91]

Hetenyi, M., 1946. Beams on Elastic Foundations. University of Michigan Press, Michigan.

Hsiung, Y.M., 2003. Theoretical elastic-plastic solution for laterally loaded piles. *Journal of Geotechnical and Geoenvironmental Engineering*, **129**(5):475-480. [doi:10.1061/(ASCE)1090-0241(2003)129:6(475)]

Hull, T.S., 1987. The Behaviour of Laterally Loaded Piles. PhD Thesis, University of Sydney, Sydney, Australia.

Kang, G.C., Song, Y.S., Kim, T.H., 2009. Behavior and stability of a large-scale cut slope considering reinforcement stages. *Landslides*, **6**(3):263-272. [doi:10.1007/s10346-009-0164-5]

Kim, B.T., Yoon, G.L., 2011. Laboratory modeling of laterally loaded pile groups in sand. *KSCE Journal of Civil Engineering*, **15**(1):65-75. [doi:10.1007/s12205-011-0924-3]

Leung, C.F., Lim, J.K., Shen, R.F., Chow, Y.K., 2003. Behavior of pile groups subjected to excavation-induced soil movement. *Journal of Geotechnical and Geoenvironmental Engineering*, **129**(1):58-65. [doi:10.1061/(ASCE)1090-0241(2003)129:1(58)]

Mokwa, R.L., 1999. Investigation of the Resistance of Pile Caps to Lateral Spreading. PhD Thesis, Department of Civil Engineering, Virginia Polytechnic Institute and State University, Blacksburg, USA.

Mokwa, R.L., Duncan, J.M., 2003. Rotational restraint of pile caps during lateral loading. *Journal of Geotechnical and Geoenvironmental Engineering*, **129**(9):829-837. [doi:10.1061/(ASCE)1090-0241(2003)129:1(58)]

Ong, D.E.L., Leung, C.F., Chow, Y.K., 2009. Behavior of pile groups subject to excavation-induced soil movement in very soft clay. *Journal of Geotechnical and Geoenvironmental Engineering*, **135**(10):1462-1474. [doi:10.

1061/(ASCE)GT.1943-5606.0000095]

Papadopoulou, M.C., Comodromos, E.M., 2010. On the response prediction of horizontally loaded fixed-head pile groups in sands. *Computers and Geotechnics*, **37**(7-8): 930-941. [doi:10.1016/j.compgeo.2010.07.011]

Poulos, H.G., 1995. Design of reinforcin piles to increase slope stability. *Canadian Geotechnical Journal*, **32**(5):808-818. [doi:10.1139/t95-078]

Poulos, H.G., Davis, E.H., 1980. Pile Foundation Analysis and Design. John Wiley & Sons, New York, NY, USA.

Rajani, B.B., Morgenstern, N.R., 1993. Pipelines and laterally loaded piles in an elasto-plastic medium. *Journal of Geotechnical Engineering*, **119**(9):1431-1447. [doi:10.1061/(ASCE)0733-9410(1993)119:9(1431)]

Randolph, M.F., 1981. The response of flexible piles to lateral loading. *Geotechnique*, **31**(2):247-259. [doi:10.1680/geot.1981.31.2.247]

Rollins, K.M., Lane, J.D., Gerber, T.M., 2005. Measured and computed lateral response of a pile group in sand. *Journal of Geotechnical and Geoenvironmental Engineering*, **131**(1):103-114. [doi:10.1061/(ASCE)1090-0241(2005)131:1(103)]

Rollins, K.M., Olsen, R.J., Egbert, J.J., Jensen, D.H., Olsen, K.G., Garrett, B.H., 2006. Pile spacing effects on lateral pile group behavior: load tests. *Journal of Geotechnical and Geoenvironmental Engineering*, **132**(10):1262-1271. [doi:10.1061/(ASCE)1090-0241(2006)132:10(1262)]

Smethurst, J.A., Powrie, W., 2007. Monitoring and analysis of the bending behaviour of discrete piles used to stabilise a railway embankment. *Geotechnique*, **57**(8):663-677. [doi:10.1680/geot.2007.57.8.663]

Won, J., Kulhawy, F.H., 2009. Reduction of pile head displacement for restrained-head single pile. *KSCE Journal of Civil Engineering*, **13**(3):143-152. [doi:10.1007/s12205-009-0143-3]

Xu, K.J., Poulos, H.G., 2000. General elastic analysis of piles and pile groups. *International Journal for Numerical and Analytical Methods in Geomechanics*, **24**(15):1109-1138. [doi:10.1002/1096-9853(20001225)24:15<1109::AID-NAG72>3.0.CO;2-N]